

# Self-similar asymptotic optical beams in semiconductor waveguides doped with quantum dots

Jun-Rong He,<sup>1,2,\*</sup> Lin Yi,<sup>1,†</sup> and Hua-Mei Li<sup>3,‡</sup>

<sup>1</sup>*Department of Physics, Huazhong University of Science and Technology, Wuhan 430074, China*

<sup>2</sup>*The School of Electronic and Information Engineering, HuBei University of Science and Technology, Xianning 437100, China*

<sup>3</sup>*Department of Physics, Zhejiang Normal University, Jinhua, Zhejiang 321004, China*

(Received 29 September 2014; revised manuscript received 6 November 2016; published 3 January 2017)

The self-similar propagation of asymptotic optical beams in semiconductor waveguides doped with quantum dots is reported. The possibility of controlling the shape of output asymptotic optical beams is demonstrated. The analytical results are confirmed by numerical simulations. We give a possible experimental protocol to generate the obtained asymptotic parabolic beams in realistic waveguides. As a generalization to the present work, the self-similar propagation of asymptotic optical beams is proposed in a power-law nonlinear medium.

DOI: [10.1103/PhysRevE.95.012202](https://doi.org/10.1103/PhysRevE.95.012202)

## I. INTRODUCTION

In nonlinear optics, the exact analytical and asymptotic similaritons in gain amplifier systems have been studied extensively due to their potential applications in nonlinearity and dispersion management systems [1–3]. These optical similaritons possess many attractive features that make them potentially useful for various applications in fiber-optic telecommunications and photonics, since they can maintain their overall shapes but allow their amplitudes and widths to change with the modulation of the system's parameters such as dispersion, nonlinearity, gain, and inhomogeneity [4,5]. It is common knowledge that the so-called self-similar solution was used in early studies as a qualitative test for the self-focusing theory and ultrashort pulse generation [6–9]. In recent years, there has been an increasing interest in the study of asymptotically exact parabolic similaritons since their first experimental realization in normally dispersive fiber amplifiers [10]. These asymptotic parabolic similaritons exist under a wide range of system parameters and exhibit some interesting properties. For instance, they can be easily generated from arbitrary input waves and their stability is guaranteed even at a high power level [11].

On the other hand, semiconductor structures with quantum dots (QDs) have been the objects of particular attention in the past several years [12]. The structures are of considerable interest from a fundamental standpoint and from the standpoint of their potential for application in new advanced optoelectronic devices. Sometimes, QDs can even change the nonlinear properties of the semiconductor media. Recently, a generic model for the quintic nonlinearity has been realized in a centrosymmetric nonlinear medium doped with resonant impurities in the limit of a large light carrier frequency detuning from the impurity resonance [13]. The resonant impurities could be rare-earth-element atoms or QDs, erbium-doped glasses, or semiconductors doped with QDs. This result provides a promising method for the investigation of self-similar optical beams in semiconductor waveguides doped with QDs.

The recent studies have paid much attention to the power-law nonlinearity in optics [14]. This type of nonlinearity can be viewed as the simplest generalization of the ubiquitous Kerr law and can model a material whose refractive index depends on the optical field amplitude raised to a power other than 2. Various semiconductors can possess power-law behavior in their refractive index, such as InSb [15], GaAs/GaAlAs [16], CdS<sub>x</sub>Se<sub>1-x</sub> [17], and liquid crystals [14]. Solitary waves in power-law nonlinearity have been investigated theoretically in the context of interface surface modes [18], elementary excitations in thin films [19], and slab (planar) waveguides [20–22]. Very recently, asymptotic compact self-similar solutions have been found in an inhomogeneous quintic nonlinear medium [23]. A most interesting issue, which is relevant to the present work, is the construction of a more general form of self-similar asymptotic solutions in power-law nonlinear media, which would have important applications in nonlinear waveguide amplifiers. Power-law nonlinearity also exists in other fields of physics such as Bose-Einstein condensates [24].

In this work we investigate the generation and propagation of self-similar asymptotic optical beams in a semiconductor waveguide doped with QDs. In Sec. II, we propose a theoretical model to describe the beam propagation in a semiconductor-QD waveguide. In Sec. III, the generation and propagation of self-similar asymptotic optical beams are investigated both analytically and numerically. As an application, in Sec. IV we give a possible experimental protocol to generate the obtained asymptotic optical beams inside realistic waveguides. In Sec. V, as the generalizations to the present work, we study the self-similar asymptotic optical beams in the power-law nonlinear media. The analytical general forms of the asymptotic optical beams are found. Finally, conclusions are presented in Sec. VI.

## II. THE MODEL

We consider the situation in which the higher-order nonlinear effect is taken into account [25] when optical beams propagate in a graded-index waveguide amplifier; i.e., the refractive index is [26]  $n(z, x) = n_0 + n_1 F(z)x^2 + n_2 I(z, x) + n_4 I(z, x)^2$ , where  $z$  is the propagation distance,  $x$  is the spatial coordinate, and  $I$  is the beam intensity. Here the first two terms describe the linear part of the refractive index and the last two terms represent the nonlinearity with  $n_2$  being the

\*jrhephysics@163.com

†yilinhust@163.com

‡lihuamei@zjnu.cn

cubic coefficient (positive  $n_2$  for self-focusing nonlinearity and negative  $n_2$  for self-defocusing nonlinearity) and  $n_4$  being the quintic coefficient that may assume positive or negative values. The term  $n_1$  is usually assumed to be positive, and the dimensionless tapering function  $F(z)$  can be negative or positive, corresponding to the graded-index waveguide acting as a focusing or defocusing lens. In experiments, the cubic-quintic nonlinearities can be obtained by doping a fiber with two appropriate semiconductor materials [27,28]. Under the paraxial and the slowly varying envelope approximations, the nonlinear wave equation governing beam propagation in a semiconductor waveguide doped with QDs can be written as

$$i \frac{\partial u}{\partial z} + \frac{1}{2k_0} \frac{\partial^2 u}{\partial x^2} + \frac{N d_{eg} \omega^2}{2\epsilon_0 k_0 c^2} \sigma_\infty + \frac{k_0 n_1}{n_0} F(z) x^2 u + \frac{k_0 n_2}{n_0} |u|^2 u + \frac{k_0 n_4}{n_0} |u|^4 u = \frac{i g(z)}{2} u, \quad (1)$$

where  $u(z, x)$  is the complex envelope of the electrical field, with  $z$  and  $x$  being the propagation distance and the spatial coordinate, respectively;  $k_0 = 2\pi n_0/\lambda$  with  $\lambda$  being the wavelength of the optical source; and  $g(z)$  is the gain (loss) coefficient. Here the third term on the left-hand side describes the nonlinear polarization due to the QDs, where  $N$  is the dopant density,  $d_{eg}$  is a dipole matrix element between the excited and ground states, and  $\sigma_\infty$  is a steady-state value of the atomic dipole moment.

According to the theory of [13], in the cw limit and assuming the light carrier frequency lies sufficiently far off resonance with the QDs, the steady-state dipole moment may be expressed as

$$\sigma_\infty \approx \frac{2d_{ge}u}{\hbar\Delta} \left( 1 - \frac{4\gamma_\perp |d_{ge}|^2 |u|^2}{\gamma_\parallel \hbar^2 \Delta^2} + \frac{16\gamma_\perp^2 |d_{ge}|^4 |u|^4}{\gamma_\parallel^2 \hbar^4 \Delta^4} \right), \quad (2)$$

where  $\gamma_\perp$  ( $\gamma_\parallel$ ) is the transverse (longitudinal) decay rate of the atomic dipole moment (inversion), and  $\Delta$  is the detuning of the incident light from QD resonance satisfying  $\Delta \gg \gamma_\perp$ . For a judicious choice of the frequency detuning  $\Delta = \sqrt{\frac{4\gamma_\perp |d_{ge}|^4 N}{\gamma_\parallel \hbar^3 \epsilon_0 n_0 |n_2|}}$ , the QD-generated and the third-order nonlinearities in Eq. (1) cancel each other, resulting in an effective renormalized quintic nonlinearity with the coefficient

$$n_{4\text{eff}} = n_4 + n_2 \sqrt[3]{\frac{4\gamma_\perp \epsilon_0^2 n_0^2 n_2^2}{\gamma_\parallel |d_{ge}|^2 N^2}}, \quad (3)$$

which is negative since  $n_2$  should be self-defocusing in the semiconductor waveguides (here,  $n_4$  may be assumed to have positive or negative values because it can be neglected in such a medium [13]).

Introducing the normalized variables  $U = (k_0 |n_{4\text{eff}}| L_D / n_0)^{1/4} u$ ,  $G(Z) = g(z) L_D$ ,  $X = x/w_0$  and  $Z = z/L_D$ , where  $w_0 = (2k_0^2 n_1 / n_0)^{-1/4}$  and  $L_D = k_0 w_0^2$  represent the characteristic transverse scale and the diffraction length, respectively, then Eq. (1) can be rewritten in a dimensionless form:

$$i \frac{\partial U}{\partial Z} + \frac{1}{2} \frac{\partial^2 U}{\partial X^2} + \frac{1}{2} F X^2 U - |U|^4 U = \frac{i G}{2} U. \quad (4)$$

It is obvious that Eq. (4) describes self-defocusing quintic nonlinearity of the waveguide, where  $F(Z)$  and  $G(Z)$  are the functions of the normalized distance  $Z$ .

### III. SELF-SIMILAR ASYMPTOTIC OPTICAL BEAMS

Our aim is to give the self-similar asymptotic parabolic solutions of Eq. (4) when the relative strength of the diffraction term is much less than that of the quintic nonlinearity. For the evolution of the optical beam to be self-similar, the functional form of the beam's intensity profile must remain unchanged at different propagation distances. Hence, one can express the beam's intensity as  $|U(Z, X)|^2 = EA(\xi)^2/\ell$ , where  $E \equiv \exp[\int_0^Z G(Z') dZ']$  describes the evolution of the peak amplitude of the beam,  $A(\xi)$  determines the evolution of the spatial profile of the beam with  $\xi \equiv X/\ell$  being the self-similarity variable, and the variable  $\ell$  is a positive function of the propagation distance  $Z$  that characterizes the change in the beam's width. As the beam width changes, its phase should contain a quadratic term  $\ell_Z X^2/(2\ell)$ , where  $\ell_Z \equiv d\ell/dZ$  and the chirp parameter is defined as the coefficient of  $X^2$ . Note that the quadratic form of the phase is a natural choice instead of an assumption [29]. Based on the above analysis, we rewrite the optical field in the following self-similar form:

$$U(Z, X) = \sqrt{\frac{E}{\ell}} A(\xi) \exp \left[ i \frac{\ell_Z}{2\ell} X^2 - i \mu \int_0^Z \frac{E^2(Z')}{\ell^2(Z')} dZ' \right], \quad (5)$$

where  $\mu$  is a positive constant. Substituting Eq. (5) into Eq. (4) and neglecting the diffraction term (the coefficient in front of the diffraction term is  $E^{-2}/2$ , vanishing at  $Z \rightarrow \infty$ ), we obtain

$$A^4 - \mu - K \xi^2 = 0, \quad (6)$$

at  $|\xi| \leq \sqrt{-\mu/K}$ , and  $A(\xi) = 0$  otherwise, where the following relations are satisfied:

$$\frac{1}{E^2} \ll 1, \quad K = \frac{\ell^3}{2E^2} (F\ell - \ell_{ZZ}), \quad (7)$$

with  $K$  being a negative constant. Note that the above reduction is essentially the same as that produced by the Thomas-Fermi approximation for the ground-state solution of the one-dimensional Gross-Pitaevskii equation with the harmonic potential [30].

Equation (6) yields a self-similar asymptotic solution

$$A^2 = \sqrt{\mu + K \xi^2}, \quad (8)$$

where constant  $\mu$  is determined by the input power:

$$P_{\text{in}} = \int_{-\infty}^{\infty} |U(0, X)|^2 dX = \int_{-\sqrt{-\mu/K}}^{\sqrt{-\mu/K}} A^2 d\xi. \quad (9)$$

To obtain the effective width of the parabolic solution, one has to solve Eq. (7). For the present situation, we consider the constants  $F$  and  $G$ . When  $F < G^2/4$ , this leads to

$$\ell = \sqrt{\frac{8K}{4F - G^2}} \exp \left( \frac{G}{2} Z \right), \quad (10)$$

When substituting Eqs. (8) and (10) into Eq. (5), one obtains the self-similar asymptotic parabolic solution for Eq. (4).

After a little algebra, we find that the effective width of the parabolic beam increases exponentially as  $\exp(GZ/2)$  while the amplitude of the parabolic beam increases exponentially as  $\exp(GZ/4)$ , and they all depend on the tapering function  $F$ . When the gain and propagation distance are given, the effective width at the asymptotic limit is increasing as  $F$  varies from negative to positive, which can be realized by the linear focusing or defocusing lens of the graded-index nonlinear waveguide. When  $F < 0$ , the larger the  $|F|$ , the smaller the effective width is and the larger the beam's amplitude; when  $F > 0$ , the effective width becomes larger when  $F$  increases, while the beam's amplitude becomes smaller. It is interesting that one may *control the shape of the output parabolic beams* by choosing an appropriate tapering parameter, since  $\ell(0)$  can vary from zero to infinity as  $F$  changes from  $-\infty$  to  $G^2/4$ . This implies that one can generate a high-power, ultrashort beam inside the waveguide with a strong enough negative tapering parameter. Note that the above parabolic solution exists when the condition  $E^2 \gg 1$  is valid. Fortunately, this condition can be easily satisfied after a short propagation distance due to the exponential increasing of  $E$ .

To check the analytical predictions, we use the Gaussian function as the input beam by resolving Eq. (4) numerically. Results for the case  $F > 0$  are shown in Fig. 1, where one can see that after about four propagation distance units, the results of numerical simulations and analytical predictions for the beam's intensity agree well with each other. Our numerical simulations are also consistent with the analytical predictions for the case  $F \leq 0$ . From Fig. 1(b) one finds that the general forms of the width and amplitude of the beam are in good agreement with the analytical results. Note that the chirp of the asymptotic parabolic solution is  $G/4$ , which is also confirmed

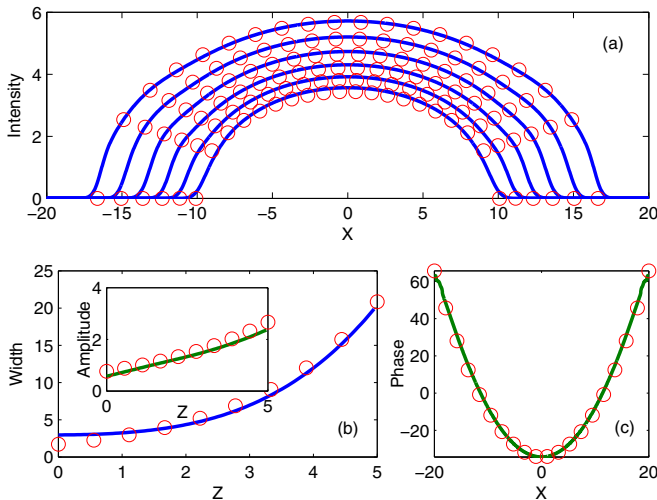


FIG. 1. (a) Characteristics of output parabolic beams in the semiconductor waveguide, starting with the Gaussian input beam  $U(0, X) = \exp(-X^2/2)/\pi^{1/4}$ . From the top to bottom, the propagation distance is  $Z = 5, 4.8, 4.6, 4.4, 4.2$ , and  $4$ , respectively. (b) The beam's width and amplitude as functions of distance  $Z$ . (c) The phase (phase offset is ignored) of the beam at propagation distance  $Z = 5$ . The solid lines and circles represent results of the direct numerical simulations of Eq. (4) and the analytical predictions, respectively. The parameters are  $G = -K = 1$ ,  $F = G^2/60$ , and  $\mu = 2/\pi$ .

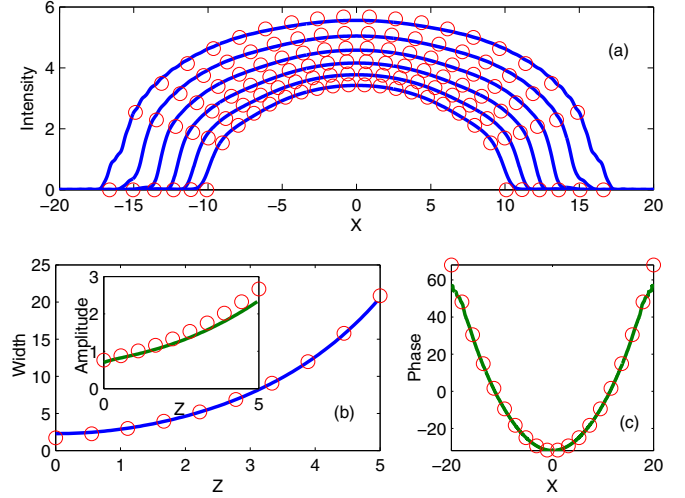


FIG. 2. The same as in Fig. 1 except that the input beam is  $U(0, X) = \text{sech}(X)/2^{1/2}$ , i.e., the hyperbolic secant input beam.

by numerical simulations [see Fig. 1(c)] using a fast phase unwrapping algorithm [31].

We have considered additional simulations that involve beams with the same input power but with different input profiles. We choose a hyperbolic secant beam,  $U(0, X) = \text{sech}(X)/2^{1/2}$ , and a super-Gaussian beam,  $U(0, X) = \exp(-X^6/2)/\{2\pi/[3\Gamma(5/6)]\}^{1/2}$ , where  $\Gamma(s)$  is a gamma function. The results of numerical simulations and analytical predictions for the general form of the beam agree well with each other; see Figs. 2 and 3. However, we find that this agreement is not as good as that in Fig. 1 after the same units of propagation distance. For the super-Gaussian input beam, Fig. 3, we notice a strong oscillatory structure on the edges of the intensity profile, which originates from the effect induced by the diffraction term in Eq. (4). This difference between the numerical and the analytical intensity profiles is connected by the existence of the diffraction term

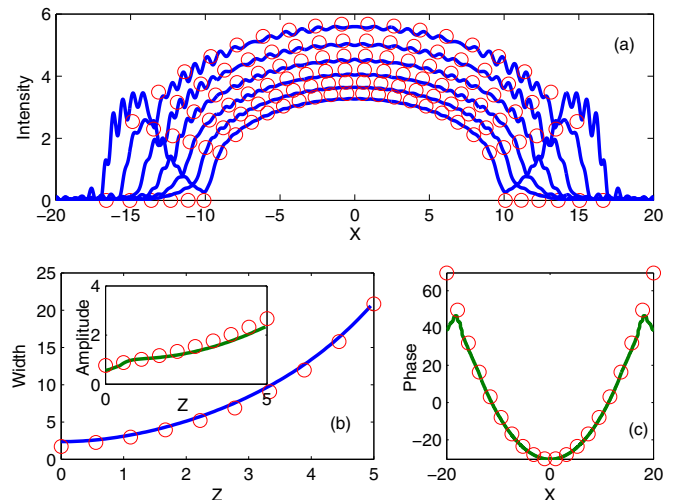


FIG. 3. The same as in Fig. 1 except that the input beam is  $U(0, X) = \exp(-X^6/2)/\{2\pi/[3\Gamma(5/6)]\}^{1/2}$ , i.e., the super-Gaussian input beam.

for the split-step Fourier method. Furthermore, one can see that the analytical predictions of the phase agree well with the numerical results only in the central region, while outside the central region it is not matched so well as the corresponding numerical profile. Therefore, we may infer that the amplifier output corresponding to the Gaussian input beam is closer to the analytical asymptotic parabolic solution than the output obtained with hyperbolic secant and super-Gaussian beam input.

It should be pointed out that we can obtain the analytical expression for the spectrum of the above asymptotic parabolic beam. Using the transformation  $\tilde{U}(Z, \Omega) = \int_{-\infty}^{\infty} U(Z, X) \exp(i\Omega X) dX / \sqrt{2\pi}$  and the stationary phase method [32], we have

$$|\tilde{U}(Z, \Omega)|^2 = \frac{2E}{G\ell} \sqrt{\mu + K \frac{\Omega^2}{\Omega_w^2}} \quad (11)$$

at  $|\Omega| \leq \Omega_w$ , and  $|\tilde{U}(Z, \Omega)|^2 = 0$  otherwise, where  $\Omega_w = G\ell/2$  and  $\Omega$  is the spatial frequency. Like the spatial distribution, the spectrum of the asymptotic parabolic beam is also a parabolic function [33,34].

#### IV. POSSIBLE EXPERIMENTAL PROTOCOL

We now give a suitable experimental protocol to generate the obtained asymptotic parabolic beams in realistic waveguides. We consider a 1- $\mu\text{m}$ -thick planar semiconductor waveguide, such as ZnSe [35], doped with CdSe QDs for  $N \approx 1 \times 10^{14} \text{ cm}^{-3}$  that are grown by molecular beam epitaxy using a thermal activation procedure [36]; we also consider a typical value of the dipole matrix element to be  $|d_{ge}| \approx 1 \times 10^{-28} \text{ C m}$  at a transition wavelength in the middle of  $\lambda \approx 500 \text{ nm}$  [37] and  $\gamma_{\perp} = 2.5\gamma_{\parallel}$  [13]. The refractive index in Eq. (1) for ZnSe can be graded with  $n_0 \approx 2.7$ ,  $n_1 \approx 0.1 \text{ cm}^{-2}$ , and  $n_2 \approx -7 \times 10^{-14} \text{ cm}^2/\text{W}$  near 500 nm [38], which leads to  $n_{4\text{eff}} \approx -1 \times 10^{-22} \text{ cm}^4/\text{W}^2$  and  $\Delta \approx 1 \times 10^{13} \text{ s}^{-1}$ . Note that the exciton lifetime of a single CdSe QD is roughly 300 ps while it is about 100 fs in bulk semiconductors [39]. Furthermore, the typical lifetimes of QDs are of the order of several tens of picoseconds [40,41]. In our situation, the semiconductor waveguide is only 1  $\mu\text{m}$  thick and confines the input beam in the  $y$  direction. Therefore, it is reasonable to assume the exciton lifetime of CdSe QDs as 100 ps in our case. This choice results in  $\gamma_{\perp} \approx 1 \times 10^{10} \text{ s}^{-1}$ , such that the system is well within the confines of a purely dispersive large-detuning regime  $\Delta \gg \gamma_{\perp}$ . In this situation,  $w_0 \approx 33 \mu\text{m}$  and the diffraction length  $L_D \approx 3.7 \text{ cm}$ . The condition  $E^2 \gg 1$  can be easily satisfied only after about one propagation distance unit ( $G = 1$ ), corresponding to a diffraction length. Furthermore, one can obtain that the required peak intensity is about  $850 \text{ MW}/\text{cm}^2$  (corresponding to the five propagation distance units in Figs. 1–3, changing into  $z \approx 18.4 \text{ cm}$ ), translating into input power levels of  $\sim 50 \text{ W}$ . Such power levels can be realized under quasi-cw conditions (such as Nd:YAG laser [34]) for which our cw theory remains applicable. Therefore, to generate asymptotic parabolic beams in realistic waveguides, one may use the frequency doubled Nd:YAG laser to produce input beams (such as Gaussian beams) which are then injected into a 18.4-cm length of CdSe/ZnSe semiconductor waveguide

with input power levels of  $\sim 50 \text{ W}$ . Measurement of the output beams of spatial and spectral profiles was then carried out using a CCD camera and spectrometer (or optical spectrum analyzer) [42,43].

#### V. GENERALIZATIONS

In this section we discuss some generalizations of Eq. (5) by considering self-similar asymptotic optical beam propagation in power-law nonlinear media. The power-law nonlinearity is introduced through a refractive index distribution [21,22]  $n(z, x) = n_0 + n_1 F(z)x^2 + n_q |u(z, x)|^q$ , where  $n_q$  is the nonlinear coefficient and the exponent may assume continuum values [21]. In this paper we only consider the case of integer values of  $q$ . The governing equation for the propagation of optical beams inside such a medium is described by

$$i \frac{\partial U}{\partial Z} + \frac{1}{2} \frac{\partial^2 U}{\partial X^2} + \frac{1}{2} F X^2 U - |U|^q U = \frac{iG}{2} U, \quad (12)$$

where the beam envelope  $U$  is normalized by  $(k_0 |n_q| L_D / n_0)^{-1/q}$ .

Employing the generalized transformation

$$U(Z, X) = \sqrt{\frac{E}{\ell}} A(\xi) \exp \left\{ i \frac{\ell_Z}{2\ell} X^2 - i\mu \int_0^Z \left[ \frac{E(Z')}{\ell(Z')} \right]^{\frac{q}{2}} dZ' \right\}, \quad (13)$$

we can reduce Eq. (12) to

$$A^q - \mu - K \xi^2 = 0, \quad (14)$$

for  $|\xi| \leq \sqrt{-\mu/K}$ , and  $A(\xi) = 0$  otherwise, when the following relations are satisfied:

$$\left( \frac{1}{E} \right)^{\frac{q}{2}} \ell^{\frac{q}{2}-2} \ll 1, \quad K = \frac{\ell}{2} \left( \frac{\ell}{E} \right)^{\frac{q}{2}} (F\ell - \ell_{ZZ}), \quad (15)$$

with  $\mu > 0$  and  $K < 0$ .

By solving the algebraic Eq. (14), a physical solution for  $A(\xi)$  is obtained:

$$A = \sqrt[q]{\mu + K \xi^2}, \quad (16)$$

where the constant  $\mu$  is determined by the input power  $P_0 = \int_{-\infty}^{\infty} |U(0, X)|^2 dX = \int_{-\infty}^{\infty} A^2 d\xi$  via the equation

$$P_0 = \frac{\Gamma(1 + \frac{2}{q}) \sqrt{\pi}}{\Gamma(\frac{3}{2} + \frac{2}{q})} \sqrt{-\frac{\mu}{K}} \mu^{\frac{2}{q}}. \quad (17)$$

It is interesting that one can obtain the curvature of  $P_0(\mu)$  as

$$\frac{d^2 P_0}{d\mu^2} = \frac{\Gamma(1 + \frac{2}{q}) \sqrt{\pi}}{\Gamma(\frac{3}{2} + \frac{2}{q})} \sqrt{-\frac{\mu}{K}} \mu^{\frac{2}{q}-2} \left( \frac{4}{q^2} - \frac{1}{4} \right), \quad (18)$$

From inspection of Eq. (18), it can be seen that the curvature is positive when  $q < q_{\text{crit}}$ , zero when  $q = q_{\text{crit}} = 4$ , and negative when  $q > q_{\text{crit}}$  [see Fig. 4(a)]. The existence of such a behavior (characterized by the change in the sign of  $d^2 P_0 / d\mu^2$ ) may suggest a proper power level when one produces beams from lasers.



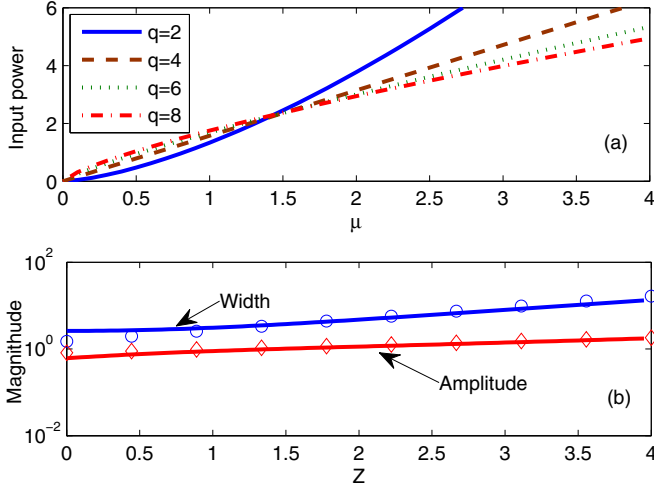


FIG. 4. (a) Beam input power  $P_0$  as a function of the parameter  $\mu$  given by Eq. (17). When  $q < 4$ , the curvature is positive,  $d^2 P_0/d\mu^2 > 0$ . For  $q = q_{\text{crit}} = 4$ ,  $P_0$  vs  $\mu$  is a straight line ( $d^2 P_0/d\mu^2 = 0$ ). When  $q > q_{\text{crit}}$ , the curvature is negative,  $d^2 P_0/d\mu^2 < 0$ . (b) Evolutions of beam width (top) and beam peak amplitude (bottom) for  $q = 6$  with the Gaussian input beam, where the gain and the tapering parameters are  $G = 1$  and  $F = G^2/10$ . The circles and squares represent results of the corresponding numerical simulations by resolving Eq. (12).

Next we consider that  $F$  and  $G$  are constants. In this case, by solving Eq. (15) we obtain the generalized effective width,

$$\ell = \left[ \frac{2K}{F - \left(\frac{q}{q+4}\right)^2 G^2} \right]^{\frac{2}{q+4}} \exp\left(\frac{q}{q+4} GZ\right), \quad (19)$$

for  $F < \left(\frac{q}{q+4}\right)^2 G^2$ .

Asymptotic parabolic solutions to Eq. (12) can also be obtained when one substitutes Eqs. (16) and (19) into Eq. (13). After some calculations, we find that the effective width of the parabolic beam increases exponentially as  $\exp\left(\frac{q}{q+4} GZ\right)$  while the amplitude of the parabolic beam increases exponentially as  $\exp\left(-\frac{2}{q+4} GZ\right)$ , and they all depend on the tapering function  $F$ . As a consequence of the exponential increase in beam width, a linear chirp is produced as  $q/[2(q+4)]$ , which is independent of the propagation distance. Similarly, the presence of a tapering parameter enables us to control the shape of the output parabolic beams, since  $\ell(0)$  can vary from zero to infinity as  $F$  changes from  $-\infty$  to  $\left(\frac{q}{q+4}\right)^2 G^2$ . The above parabolic solution exists when the first condition in Eq. (15) is valid. We find that this condition can be more easily satisfied when  $q$  increases, for the same gain  $G$ . For example, when  $G = 1$ , the diffraction term in Eq. (12) can be neglected after about 1.6 propagation distances for  $q = 2$  while it can be neglected after about only one propagation distance for  $q = 4$ . As  $q$  increases, this propagation distance becomes shorter and shorter. This implies that the self-similar solutions in power-law nonlinear media with higher exponent could more rapidly evolve into the parabolic profiles than the lower one.

Figure 4(b) presents an example of the evolution of beam width and beam peak amplitude in both numerical and

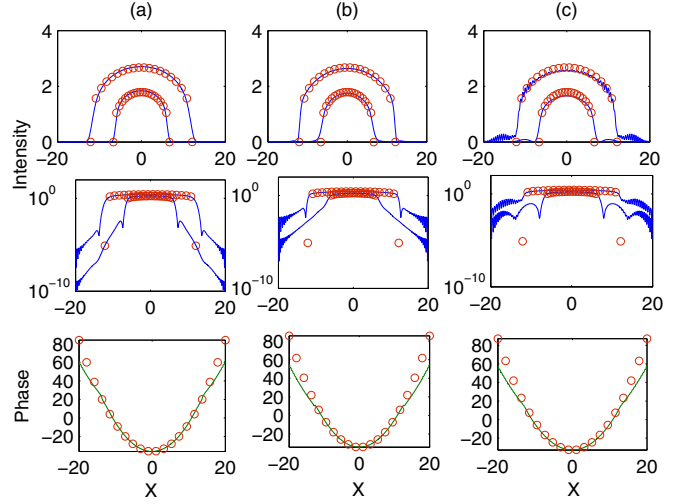


FIG. 5. Characteristics of output parabolic beams for  $q = 6$  with (a) Gaussian (left column), (b) hyperbolic secant (middle column), and (c) super-Gaussian (right column) profiles, which are of the same initial power  $P_0 = 1$ . The top and middle rows show the distributions of intensity profiles on a linear scale and on a logarithmic scale, respectively (the upper lines represent propagation distance at  $Z = 4$  while the bottom lines represent propagation distance at  $Z = 3$ ). The bottom row shows the corresponding phase distributions of the output beams at  $Z = 4$ . The solid lines and circles represent results of the direct numerical simulations of Eq. (12) and the analytical predictions, respectively. The parameters are  $G = -K = 1$ ,  $F = G^2/10$ , and  $\mu = 0.5356$ .

analytical profiles for  $q = 6$  with the Gaussian input beam, where the direct numerical simulation of Eq. (12) agrees quite well with the asymptotic analytical predictions. Figure 5 shows the evolutions of input beams with different profiles and the corresponding analytical predictions. Since they have the same initial power, they all converge to the parabolic beam. One can find that the general form of the envelope profile and the phase agree well with the analytical predictions.

## VI. CONCLUSIONS

In conclusion, we have studied the propagation properties of asymptotic optical beams in semiconductor waveguides doped with QDs. The possibility of controlling the shape of output asymptotic optical beams was demonstrated. The analytical results have been confirmed by numerical simulations. We also gave a possible experimental protocol to generate the obtained asymptotic parabolic beams in realistic waveguides. Finally, as the generalization to the present work, we have investigated the self-similar propagation of asymptotic optical beams in the power-law nonlinear media.

## ACKNOWLEDGMENT

This work was supported by the National Special Plan Project of China under Grant No. 0262012011 and the National Natural Science Foundation of China under Grant No. 11675146.

- [1] G. P. Agrawal, *Nonlinear Fiber Optics*, 4th ed. (Academic Press, New York, 2007).
- [2] J. D. Moores, *Opt. Lett.* **21**, 555 (1996).
- [3] S. Chen and J. M. Dudley, *Phys. Rev. Lett.* **102**, 233903 (2009).
- [4] B. S. Azimov, M. M. Sagatov, and A. P. Sukhorukov, *Sov. J. Quantum Electron.* **21**, 785 (1991).
- [5] V. N. Serkin, A. Hasegawa, and T. L. Belyaeva, *J. Mod. Opt.* **57**, 1456 (2010).
- [6] V. I. Talanov, *Radiophys. Quantum Electron.* **9**, 260 (1966).
- [7] V. I. Talanov, *JETP Lett.* **11**, 199 (1970).
- [8] J. H. Marburger, *Prog. Quantum Electron.* **4**, 35 (1975).
- [9] E. G. Lariontsev and V. N. Serkin, *Sov. J. Quantum Electron.* **5**, 796 (1975).
- [10] M. E. Fermann, V. I. Kruglov, B. C. Thomsen, J. M. Dudley, and J. D. Harvey, *Phys. Rev. Lett.* **84**, 6010 (2000).
- [11] J. M. Dudley, C. Finot, D. J. Richardson, and G. Millot, *Nat. Phys.* **3**, 597 (2007).
- [12] D. Bimberg, M. Grundmann, and N. N. Ledentsov, *Quantum Dot Heterostructures* (Wiley, Chichester, UK, 1999).
- [13] S. A. Ponomarenko and S. Haghighi, *Phys. Rev. A* **81**, 051801(R) (2010).
- [14] D. Mihalache, M. Bertolotti, and C. Sibilia, *Prog. Opt.* **27**, 227 (1989).
- [15] J. G. H. Mathew, A. K. Kar, N. R. Heckenberg, and I. Galbraith, *IEEE J. Quantum Electron.* **21**, 94 (1985).
- [16] D. S. Chemla, D. A. B. Miller, and P. W. Smith, *Opt. Eng.* **24**, 556 (1985).
- [17] R. K. Jain and R. C. Lind, *J. Opt. Soc. Am.* **73**, 647 (1983); S. S. Yao *et al.*, *Appl. Phys. Lett.* **46**, 801 (1985).
- [18] A. W. Snyder and H. T. Tran, *Opt. Commun.* **98**, 309 (1993).
- [19] C. T. Seaton *et al.*, *IEEE J. Quantum Electron.* **21**, 774 (1985).
- [20] G. I. Stegeman *et al.*, *IEEE J. Quantum Electron.* **22**, 977 (1986); U. Langbein, F. Lederer, and H. Ponath, *Opt. Commun.* **53**, 417 (1985); L. Wu, *ibid.* **224**, 51 (2003).
- [21] A. W. Snyder and D. J. Mitchell, *Opt. Lett.* **18**, 101 (1993).
- [22] R. W. Micallef, V. V. Afanasjev, Y. S. Kivshar, and J. D. Love, *Phys. Rev. E* **54**, 2936 (1996).
- [23] J. R. He, L. Yi, and H. M. Li, *Phys. Rev. E* **90**, 013202 (2014).
- [24] V. A. Brazhnyi, V. V. Konotop, and L. P. Pitaevskii, *Phys. Rev. A* **73**, 053601 (2006).
- [25] G. I. Barenblatt, *Scaling, Self-Similarity, and Intermediate Asymptotics* (Cambridge University Press, Cambridge, UK, 1996).
- [26] J. D. He and J. F. Zhang, *J. Phys. A: Math. Theor.* **44**, 205203 (2011).
- [27] J. Herrmann, *Opt. Commun.* **87**, 161 (1992).
- [28] C. De Angelis, *IEEE J. Quantum Electron.* **30**, 818 (1994).
- [29] L. Wu, J. F. Zhang, L. Li, Q. Tian, and K. Porsezian, *Opt. Express* **16**, 6352 (2008); L. Wu, L. Li, and J. F. Zhang, *Phys. Rev. A* **78**, 013838 (2008).
- [30] F. Dalfó, S. Giorgini, L. P. Pitaevskii, and S. Stringari, *Rev. Mod. Phys.* **71**, 463 (1999).
- [31] M. A. Schofield and Y. M. Zhu, *Opt. Lett.* **28**, 1194 (2003).
- [32] R. Rolleston and N. George, *J. Opt. Soc. Am. A* **4**, 148 (1987).
- [33] V. I. Kruglov, A. C. Peacock, J. M. Dudley, and J. D. Harvey, *Opt. Lett.* **25**, 1753 (2000).
- [34] V. I. Kruglov, A. C. Peacock, J. D. Harvey, and J. M. Dudley, *J. Opt. Soc. Am. B* **19**, 461 (2002).
- [35] S. R. Skinner, G. R. Allan, D. R. Andersen, and A. L. Smirl, *IEEE J. Quantum Electron.* **27**, 2211 (1991).
- [36] M. Rabe, M. Lowisch, and F. Henneberger, *J. Cryst. Growth* **184–185**, 248 (1998).
- [37] K. Watanabe, H. Nakano, A. Honold, and Y. Yamamoto, *Phys. Rev. Lett.* **62**, 2257 (1989).
- [38] G. R. Allan, S. R. Skinner, D. R. Andersen, and A. L. Smirl, *Opt. Lett.* **16**, 156 (1991).
- [39] T. Flissikowski, A. Hundt, M. Lowisch, M. Rabe, and F. Henneberger, *Phys. Rev. Lett.* **86**, 3172 (2001).
- [40] N. H. Bonadeo, J. Erland, D. Gammon, D. Park, D. S. Katzer, and D. G. Steel, *Science* **282**, 1473 (1998).
- [41] G. Panzarini, U. Hohenester, and E. Molinari, *Phys. Rev. B* **65**, 165322 (2002).
- [42] Xinkui He, M. Miranda, J. Schwenke, O. Guilbaud, T. Ruchon, C. Heyl, E. Georgadiou, R. Rakowski, A. Persson, M. B. Gaarde, and A. L'Huillier, *Phys. Rev. A* **79**, 063829 (2009).
- [43] R. Machulka, J. Svozilík, J. Soubusta, J. Peřina, Jr., and O. Haderka, *Phys. Rev. A* **87**, 013836 (2013).